National Conference with International Participation
ENGINEERING MECHANICS 2006
Svratka, Czech Republic, May 15 – 18, 2006
paper no. 135

ELASTIC CYLINDER WITH MICROSTRUCTURE

V. Nováček, R. Cimrman, J. Rosenberg [1]

Summary: *This paper is concerned with the modelling of a microstretch elastic solids. In contrast to the classical theory of continuum, the points of the microstretch material can also rotate and deform independently of their translations. The microstructure is thus characterized by the additional degrees of freedom. The analytical solution for the problem of extension for a homogeneous and isotropic microstretch cylinder is known. It is compared to the results of numerical simulations using finite element method.*

1. Introduction

Standard continuum mechanics studies the problems in which the microstructure is homogenized by phenomenological averages. Functions that characterize continuum variables and quantities are assumed to be smooth a continuous in space and time. Distributions of stresses, strains and other quantities and the material itself within an infinitesimal material neighbourhood of a typical particle (or material element) are regarded as essentially uniform. However, the microscale, often very complicated, is not uniform in general. Framework of the standard continuum mechanics does not respect in principle the inner material structure. Classical elasticity becomes inaccurate when the length scales of structure constituents become comparable to some intrinsic characteristic length scale of the material. Various approaches are studied to cope this problem, e.g. homogenization, higher grade theories and higher order theories. Microcontinuum theory belongs among the last mentioned.

The general idea of the microcontinual approach is based on the introduction of some additional fields (degrees of freedom) that characterize the behaviour of the microstructure. One particular case is the micromorphic model introduced and studied e.g. in Capriz [1989]; Eringen [1999]. In the case of micromorphic continuum, each point of the continuum can translate, rotate and deform. In Eringen [1999], each point is associated with a triple of vectors, the so-called directors, that can rotate and deform; they characterize the intrinsic deformation of the microstructure. In Capriz [1989], an order parameters' manifold is associated with the body.

[1] Ing. Vít Nováček, Ing. Robert Cimrman, Ph.D., Prof. Ing. Josef Rosenberg, DrSc., Department of Mechanics, Faculty of Applied Sciences, University of West Bohemia, Univerzitní 8, 306 14 Plzeň, phone: +420 377 63 4709, e-mail: vnovacek@kme.zcu.cz

This manifold is a space of second order tensors with positive determinant in the case of micromorphic continuum. Both approaches are formally identical. Microstretch continuum is a subset of the micromorphic one, where the points can rotate and deform uniformly (contract and/or stretch) without microshear. Porous and granular materials and biological tissues may be descibed with this model. The points of micropolar continuum can rotate without deformation. It is a convenient description for polar materials such as liquid crystals.

This paper deals with the modelling of the microstretch lineraly elastic cylinder. The authors of this paper provide the variational, weak and numerical formulation and the discretization of the problem of linearly elastic microstretch solid in three dimensions, as well as the finite element package solving this problem. The aim of this article is to compare the results from the numerical simulations with the known analytical solution. The analytical solution for the problems of extension and bending for a homogeneous and isotropic microstretch cylinder is shown in Ieşan and Nappa [1995] and for the torsion and flexure in De Cicco and Nappa [1997].

Section 2. presents the basic equations that characterize the boundary value problem of the microstretch linearly elastic isotropic solid body. Weak formulation is presented as well. Section 3. describes briefly the analitycal solution of the extension problem of the microstretch cylinder. Section 4. presents in detail the finite element discretization of the problem of the microstretch linearly elastic isotropic solid body in three dimensions. Section 5. presents the results of the numerical simulation of the extension problem of microstretch cylinder, compares the results with the prediction of the theoretical solution and discuss the results. Section 6. gives a conclusion of the paper.

2. Basic equations

Let us denote $\mathcal{B}$ the placement of the body under consideration in the three-dimensional Euclidean space so that $\mathcal{B}$ is the set of all places $\mathbf{x}$ occupied by the body at time t. We denote $\mathcal{B}_0$ the reference placement and it is the set of all places $\mathbf{X}$ occupied by the body at time $t = 0$. We assume the Cartesian coordinate system throughout this paper. Comma denotes a partial differentiation with respect to appropriate coordinate. Linear microstretch continuum is characterized by three independent kinematical fields: displacement field $\mathbf{u} = \mathbf{x} - \mathbf{X}$, field of microscopical rotations $\boldsymbol{\phi}$ and microstrech function ψ which is a scalar function. Linear strain tensors are introduced in Eringen [1999] as

$$\varepsilon_{kl} = u_{l,k} + \epsilon_{lkm}\phi_m, \quad \kappa_{kl} = \phi_{k,l}, \quad \gamma_k = 3\phi_{,k}, \quad e = 3\psi. \tag{1}$$

Balance equations comprise

$$t_{kl,k} = 0, \quad m_{kl,k} + \epsilon_{lmn}t_{mn} = 0, \quad h_{k,k} - s = 0, \tag{2}$$

where we omitted the body loads for abbreviation. t_{kl} denotes the Cauchy stress tensor that is, in general, non-symmetric. h_k is the microstretch vector (sometimes called hyperstress) and m_{kl} is the couple stress tensor. The couple stress tensor divergence is compensated by the non-symmentric part of the macroscopic stress tensor, while s compensates the divergence of the hyperstress and represents the net pressure involved in the dilatation of the microstructure. Its

origin is in the difference between traces of the macroscopic stress tensor and the microstress average, see Eringen [1999]. Constitutive relations of microstrech isotropic solid are following

$$\begin{aligned} t_{kl} &= (\lambda_0\psi + \lambda\varepsilon_{mm})\delta_{kl} + (\mu+\kappa)\varepsilon_{kl} + \mu\varepsilon_{lk}, \\ m_{kl} &= \alpha\kappa_{mm}\delta_{kl} + \beta\kappa_{kl} + \gamma\kappa_{lk} + (1/3)b_0\epsilon_{mlk}\gamma_m, \\ h_k &= a_0\gamma_k + b_0\epsilon_{klm}\kappa_{lm}, \\ s &= \lambda_1\psi + \lambda_0\varepsilon_{kk}, \end{aligned} \tag{3}$$

with 10 material moduli λ, μ, κ, α, β, γ, λ_0, λ_1, a_0 and b_0. Denoting $\tilde{t}_i$ the surface traction, $\tilde{m}_i$ the surface moment and $\tilde{h}$ the microtraction, we may write the boundary conditions at regular points of $\partial\mathcal{B}$ as

$$\tilde{t}_i = t_{ji}n_j, \quad \tilde{m}_i = m_{ji}n_j, \quad \tilde{h} = h_i n_i. \tag{4}$$

We are limited to the linear theory so that the internal energy density is assumed to be a positive definite quadratic form. Material stability requires that the material moduli fullfil the restrictions

$$\begin{gathered} 3\lambda + 2\mu + \kappa \geq 0, \quad 3\alpha + \beta + \gamma \geq 0, \\ 2\mu + \kappa \geq 0, \quad \gamma + \beta \geq 0, \quad \gamma - \beta \geq 0, \quad \kappa \geq 0, \\ 3\lambda + 2\mu + \kappa \geq 3\lambda_0^2/\lambda_1, \quad a_0 \geq 0, \quad \lambda_1 > 0. \end{gathered} \tag{5}$$

The variational formulation of the boundary value problem for linearly elastic microstretch body in three dimensions may be expressed as

$$\int_\Omega t_{ij,j}\delta u_j d\Omega + \int_\Omega (m_{ij,i} + \epsilon_{jkl}t_{kl})\delta\phi_j d\Omega + \int_\Omega (h_{i,i} - s)\delta\psi d\Omega = 0, \tag{6}$$

with the boundary terms omitted for brevity and Ω being an arbitrary sub-volume of the body $\mathcal{B}$ and δ denoting the variation with respect to the corresponding variable. Applying the Green Theorem we obtain the weak formulation

$$\int_\Omega t_{ij}(\delta u_j)_{,i} d\Omega + \int_\Omega m_{ij}(\delta\phi_j)_{,i} d\Omega - \int_\Omega \epsilon_{jkl}t_{kl}\delta\phi_j d\Omega + \int_\Omega h_i(\delta\psi)_{,i} d\Omega + \int_\Omega s\delta\psi d\Omega = 0, \tag{7}$$

valid $\forall\delta u_i, \delta\phi_i, \delta\psi$ and $\forall\Omega$.

3. Microstretch cylinder

The analytical solution for the problems of extension and bending for a homogeneous and isotropic microstretch cylinder is shown in Ieşan and Nappa [1995]. This problem was solved for constitutive relations without the coupling terms with material parameter b_0. These two terms (see (3)) were introduced later in Eringen [1999]. The solution of three dimensional problem is based on the solutions of three auxiliary plane strain problems, see e.g. Ieşan and Nappa [1994].

We consider a cylinder of isotropic material which occupies the region $\mathcal{B}$ whose boundary is $\partial\mathcal{B}$. We assume that the cylinder is bounded by plane ends perpendicular to the generators.

The generic cross-section Σ is assumed to be a simply-connected regular region bounded by the closed curve L. The axis Ox_3 of our coordinate system will be directed parallel to the generators of the cylinder. The cylinder is assumed to be of length l and one of its bases is taken to lie in the x_1Ox_2 plane while the other is in the plane $x_3 = l$. We denote by S the lateral surface of the cylinder. The cylinder is assumed to be free from lateral loadings.

Let us consider the extension of the microstretch cylinder. The loading applied on the end $x_3 = l$ is assumed to be statically equivalent to a force $\mathbf{F} = [0, 0, F_3]^T$. The solution of the extension problem is

$$u_1 = \frac{F_3}{EA}\nu_1 x_1, \quad u_2 = \frac{F_3}{EA}\nu_1 x_2, \quad u_3 = -\frac{F_3}{EA}x_3, \quad \phi_k = 0, \quad \psi = \frac{F_3}{EA}\nu_2, \tag{8}$$

where A is the cross-section of the cylinder and

$$\begin{aligned} E &= \lambda + 2\mu + \kappa - 2\lambda\nu_1 - \lambda_0\nu_2, \\ \nu_1 &= (\lambda - \lambda_0^2/\lambda_1)/(2\lambda + 2\mu + \kappa - 2\lambda_0^2/\lambda_1), \\ \nu_2 &= (1 - 2\nu_1)\lambda_0/\lambda_1. \end{aligned} \tag{9}$$

Other types of loading may be considered too. We have tried the simulations with the bending of the cylinder, however, the results were not satisfactory. After discussion with proffessor Ieşan we have found that there are typesetting errors in the analytical solution for bending in Ieşan and Nappa [1995]. Recently, we have received the corrected version and the bending of the cylinder is studied intensively.

4. Finite element discretization

We use the following notation for the discrete counterparts of the microstretch quantities restricted to a finite element e: strain $\boldsymbol{\varepsilon}^e$, torsion-curvature $\boldsymbol{\kappa}^e$, macroscopic stress $\boldsymbol{t}^e$,couple stress $\boldsymbol{m}^e$, hyperstress $\boldsymbol{h}^e$ and net pressure $\boldsymbol{s}^e$. The discretized rank-2 tensors are stored as vectors, using the following ordering

$$\bullet_{ij} = \begin{bmatrix} \bullet_{11} & \bullet_{12} & \bullet_{13} \\ \bullet_{21} & \bullet_{22} & \bullet_{23} \\ \bullet_{31} & \bullet_{32} & \bullet_{33} \end{bmatrix} \approx \begin{bmatrix} \bullet_{11} & \bullet_{22} & \bullet_{33} & \bullet_{12} & \bullet_{13} & \bullet_{23} & \bullet_{21} & \bullet_{31} & \bullet_{32} \end{bmatrix}^T , \tag{10}$$

i.e. we store first the diagonal, then the upper triangle and finally the lower triangle. Let us denote by $\boldsymbol{\varphi}$ the $(n \times 1)$ vector of element restrictions of the base functions and by $\boldsymbol{G}_i$, $i = 1, \ldots, 3$ their derivatives with respect to the space coordinates x_i. Let $\boldsymbol{u}^e$, $\boldsymbol{\phi}^e$, $\boldsymbol{\psi}^e$ be the vectors of displacements, microrotations, and microstretch of element nodes respectively and $\boldsymbol{d}^e = [\boldsymbol{u}^e, \boldsymbol{\phi}^e, \boldsymbol{\psi}^e]^T$ the compound vector of element unknowns. We also denote a k-dimensional identity matrix by $\boldsymbol{I}_k$. The constitutive equations for an isotropic microstretch material (3), in the discrete form can be written in general as

$$\bullet^e = \boldsymbol{D}_\bullet \boldsymbol{B} \boldsymbol{d}^e , \tag{11}$$

where $\bullet \in \{\boldsymbol{t}, \boldsymbol{m}, \boldsymbol{h}, \boldsymbol{s}\}$. The particular forms of $\boldsymbol{D}_\bullet$, $\boldsymbol{B}$ are described below. Here $\boldsymbol{u}^e = [\boldsymbol{u}_1^e, \boldsymbol{u}_2^e, \boldsymbol{u}_3^e]^T$, $\boldsymbol{\phi}^e = [\boldsymbol{\phi}_1^e, \boldsymbol{\phi}_2^e, \boldsymbol{\phi}_3^e]^T$ and thus $\boldsymbol{d}^e$ has length $7n$, where n is the number of element

nodes. The element approximations of unknown fields are then $u_i \approx \boldsymbol{\varphi}^T \boldsymbol{u}_i^e$, $\phi_i \approx \boldsymbol{\varphi}^T \boldsymbol{\phi}_i^e$, $i = 1, 2, 3$, $\psi \approx \boldsymbol{\varphi}^T \boldsymbol{\psi}^e$ and their derivatives $u_{i,j} \approx \boldsymbol{G}_j \boldsymbol{u}_i^e$, $\phi_{i,j} \approx \boldsymbol{G}_j \boldsymbol{\phi}_i^e$, $\psi_{,j} \approx \boldsymbol{G}_j \boldsymbol{\psi}^e$. The element restrictions of approximations of strain measures stored as vectors can be expressed as follows (see (1)):

$$\boldsymbol{\varepsilon}^e = \left[\begin{array}{c} u_{1,1} \\ u_{2,2} \\ u_{3,3} \\ \hline u_{2,1} \\ u_{3,1} \\ u_{3,2} \\ \hline u_{1,2} \\ u_{1,3} \\ u_{2,3} \end{array}\right] + \left[\begin{array}{c} 0 \\ 0 \\ 0 \\ \hline -\phi_3 \\ \phi_2 \\ -\phi_1 \\ \hline \phi_3 \\ -\phi_2 \\ \phi_1 \end{array}\right] \approx \underbrace{\left[\begin{array}{ccc|ccc} \boldsymbol{G}_1 & & & & & \\ & \boldsymbol{G}_2 & & & & \\ & & \boldsymbol{G}_3 & & & \\ \hline \boldsymbol{G}_1 & & & & & -\boldsymbol{\varphi}^T \\ & \boldsymbol{G}_1 & & & \boldsymbol{\varphi}^T & \\ & \boldsymbol{G}_2 & & -\boldsymbol{\varphi}^T & & \\ \hline \boldsymbol{G}_2 & & & & & \boldsymbol{\varphi}^T \\ \boldsymbol{G}_2 & & & & -\boldsymbol{\varphi}^T & \\ & \boldsymbol{G}_3 & & \boldsymbol{\varphi}^T & & \end{array}\right]}_{\equiv [\boldsymbol{G}^\dagger | \boldsymbol{\nu}]} \cdot \left[\begin{array}{c} \boldsymbol{u}^e \\ \boldsymbol{\phi}^e \end{array}\right], \tag{12}$$

$$\boldsymbol{\kappa}^e = \left[\begin{array}{c} \phi_{1,1} \\ \phi_{2,2} \\ \phi_{3,3} \\ \hline \phi_{1,2} \\ \phi_{1,3} \\ \phi_{2,3} \\ \hline \phi_{2,1} \\ \phi_{3,1} \\ \phi_{3,2} \end{array}\right] \approx \underbrace{\left[\begin{array}{ccc} \boldsymbol{G}_1 & & \\ & \boldsymbol{G}_2 & \\ & & \boldsymbol{G}_3 \\ \hline \boldsymbol{G}_2 & & \\ \boldsymbol{G}_2 & & \\ & \boldsymbol{G}_3 & \\ \hline & \boldsymbol{G}_1 & \\ & & \boldsymbol{G}_1 \\ & & \boldsymbol{G}_2 \end{array}\right]}_{\equiv \boldsymbol{G}} \cdot \boldsymbol{\phi}^e \,, \qquad \left[\begin{array}{c} \psi_{,1} \\ \psi_{,2} \\ \psi_{,3} \end{array}\right] \approx \underbrace{\left[\begin{array}{c} \boldsymbol{G}_1 \\ \boldsymbol{G}_2 \\ \boldsymbol{G}_3 \end{array}\right]}_{\equiv \boldsymbol{G}_c} \cdot \boldsymbol{\psi}^e \,. \tag{13}$$

The matrices $\boldsymbol{D}_\bullet$, $\boldsymbol{B}$ of (11) are in this case

$$\left[\begin{array}{c} \boldsymbol{D_t} \\ \boldsymbol{D_m} \\ \boldsymbol{D_h} \\ \boldsymbol{D_s} \end{array}\right] \equiv \left[\begin{array}{cccc} \boldsymbol{D}_1 & \boldsymbol{D}_1 & \lambda_0 \mathbf{1}_9 & \\ & & \boldsymbol{D}_2 & b_0 \boldsymbol{P}^T \\ & & b_0 \boldsymbol{P} & a_0 \boldsymbol{I}_3 \\ \lambda_0 \mathbf{1}_9^T & \lambda_0 \mathbf{1}_9^T & \lambda_1 & \end{array}\right], \quad \boldsymbol{B} \equiv \left[\begin{array}{ccc} \boldsymbol{G}^\dagger & & \\ & \boldsymbol{\nu} & \\ & \boldsymbol{G}^\dagger & \\ & & \boldsymbol{\varphi}^T \\ & & \boldsymbol{G}_c \end{array}\right], \tag{14}$$

where the (3×9) matrix $\boldsymbol{P}$

$$\boldsymbol{P} \equiv \left[\begin{array}{ccc|ccc} & & & & & 1 \\ & & -1 & & -1 & \\ & 1 & & 1 & & \\ \hline -1 & & & & & \end{array}\right] \tag{15}$$

corresponds to the alternating symbol ϵ_{ijk}, $\mathbf{1}_9 \equiv [1, 1, 1 | 0, 0, 0 | 0, 0, 0]^T$ and $\boldsymbol{D}_1$, $\boldsymbol{D}_2$ are described below. First we define a transposition operator $\boldsymbol{J}_9$ acting on tensors stored as $(9 \times *)$ matrices as given by relations $\boldsymbol{\nu}^\dagger = \boldsymbol{J}_9 \boldsymbol{\nu} (= -\boldsymbol{\nu})$, $\boldsymbol{G}^\dagger = \boldsymbol{J}_9 \boldsymbol{G}$; the † upper right index means transposition of the original matrix-like tensor. Then we can define

$$\boldsymbol{D}_1 = \lambda \mathbf{1}_9 \mathbf{1}_9^T + (\mu + \kappa) \boldsymbol{I}_9 + \mu \boldsymbol{J}_9 \,, \quad \boldsymbol{D}_2 = \alpha \mathbf{1}_9 \mathbf{1}_9^T + \beta \boldsymbol{J}_9 + \gamma \boldsymbol{I}_9 \,. \tag{16}$$

The discrete version of the variational formulation (7), restricted to e, is

$$
\begin{aligned}
&(\delta\boldsymbol{u}^e)^T \left[\int_e \boldsymbol{G}^{\dagger T}\boldsymbol{D_t}\boldsymbol{B}\,\mathrm{d}e\right]\boldsymbol{d}^e \\
+&(\delta\boldsymbol{\phi}^e)^T \left[\int_e (\boldsymbol{G}^{\dagger T}\boldsymbol{D_m}+\boldsymbol{\nu}^T\boldsymbol{D_t})\boldsymbol{B}\,\mathrm{d}e\right]\boldsymbol{d}^e \\
+&(\delta\boldsymbol{\psi}^e)^T \left[\int_e (\boldsymbol{G}_c^T\boldsymbol{D_h}+\boldsymbol{\varphi}\boldsymbol{D_s})\boldsymbol{B}\,\mathrm{d}e\right]\boldsymbol{d}^e \overset{\text{assemble}}{\longrightarrow} 0 \quad \forall\delta\boldsymbol{u},\delta\boldsymbol{\phi},\delta\boldsymbol{\psi}\ .
\end{aligned}
\tag{17}
$$

Hence it is easy to see that the element matrix is symmetric and has the following structure:

$$
\boldsymbol{K}^e \equiv \left[\begin{array}{c|c|c}
\boldsymbol{G}^{\dagger T}\boldsymbol{D}_1\boldsymbol{G}^{\dagger} & \boldsymbol{G}^{\dagger T}\boldsymbol{D}_1\boldsymbol{\nu} & \boldsymbol{G}^{\dagger T}\lambda_0\mathbf{1}_9\boldsymbol{\varphi}^T \\ \hline
\boldsymbol{\nu}^T\boldsymbol{D}_1\boldsymbol{G}^{\dagger} & \boldsymbol{\nu}^T\boldsymbol{D}_1\boldsymbol{\nu}+\boldsymbol{G}^{\dagger T}\boldsymbol{D}_2\boldsymbol{G}^{\dagger} & \boldsymbol{\nu}^T\lambda_0\mathbf{1}_9\boldsymbol{\varphi}^T+\boldsymbol{G}^{\dagger T}b_0\boldsymbol{P}^T\boldsymbol{G}_c \\ \hline
\boldsymbol{\varphi}\lambda_0\mathbf{1}_9^T\boldsymbol{G}^{\dagger} & \boldsymbol{\varphi}\lambda_0\mathbf{1}_9^T\boldsymbol{\nu}+\boldsymbol{G}_c^T b_0\boldsymbol{P}\boldsymbol{G}^{\dagger} & \boldsymbol{\varphi}\lambda_1\boldsymbol{\varphi}^T+\boldsymbol{G}_c^T a_0\boldsymbol{I}_3\boldsymbol{G}_c
\end{array}\right]\ . \tag{18}
$$

This block structure is also reflected in the assembled tangent stiffness matrix. Let us recapitulate the sizes of the involved matrices:

matrix	$\boldsymbol{\varphi}$	$\boldsymbol{G}^{\dagger}$	$\boldsymbol{G}_c$	$\boldsymbol{\nu}$	$\boldsymbol{D}_1$	$\boldsymbol{D}_2$	$\boldsymbol{P}$	$\boldsymbol{K}^e$
rows	n	9	3	9	9	9	3	$3n+3n+n$
columns	1	$3n$	n	$3n$	9	9	9	$3n+3n+n$

It is worth noting that the stiffness matrix is indefinite and thus we are obliged use a robust direct solver, e.g. UMFPACK (see Davis [2004]) for the resolution of the linear system.

5. Results and discussion

We study the extension of the cylinder described above with radius $r = 0.25$ and length $l = 2$. The $x_3 = 0$ plane is fixed while on the $x_3 = l$ plane the loading is applied. More precisely, nodal displacements $u_3 = 0$ are set to zero on the $x_3 = 0$ plane while the central node with the coordinates $[0, 0, 0]^T$ is fixed in all three (macroscopic) directions, i.e. $u_i = 0$, $i = 1, 2, 3$ is prescribed for this node. In the case of extension, the microrotations are fixed for all nodes of the body, i.e. $\phi_i = 0$, $i = 1, 2, 3$. Pressure is prescribed on the $x_3 = l$ plane equivalent to F_3/A value. Three dimensional mesh was constructed in Gambit, our finite element package was used for computations and the results are visualized in ParaView software. Material parameters were chosen so that the thermodynamical restrictions were fulfiled and with $b_0 = 0$ according to the case studied in Ieşan and Nappa [1995]. Figure 1 presents the comparision of the results from simulation with values predicted by theory. The $x_3 = l$ was loaded with the pressure $F_3/A = 20.000$. Figure 2 presents the comparision of the numerical and theoretical results for various boundary conditions (pressure prescribed) as the dependence between the displacement u_z of the loaded plane $x_3 = l$ and the pressure applied on that plane.

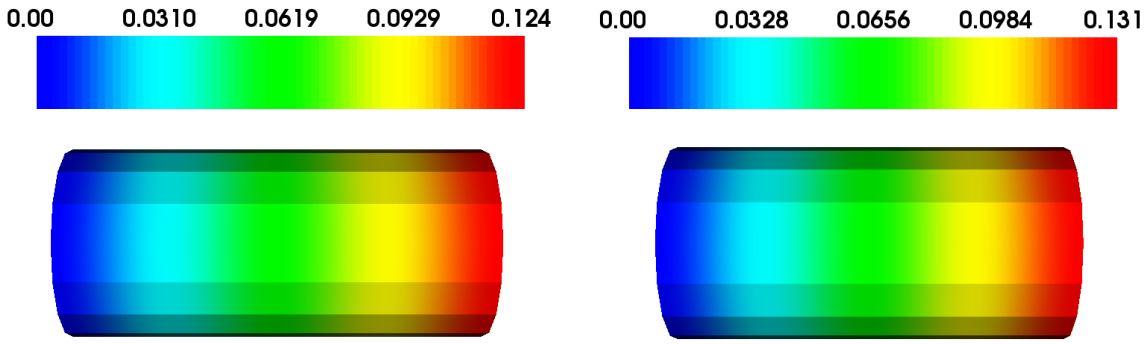

(a) simulation (b) theory

Figure 1: Distribution of the u_z displacement field, pressure 20.000 applied.

We are limited to the linear theory, of course, the dependence is linear. There is an apparent discrepancy between the value predicted by theory and the result of the numerical simulation from the applied pressure value 14.000. We may assume that from this point, the deformation is no longer linear and model cannot give good results. Up to this value, the results are satisfactory.

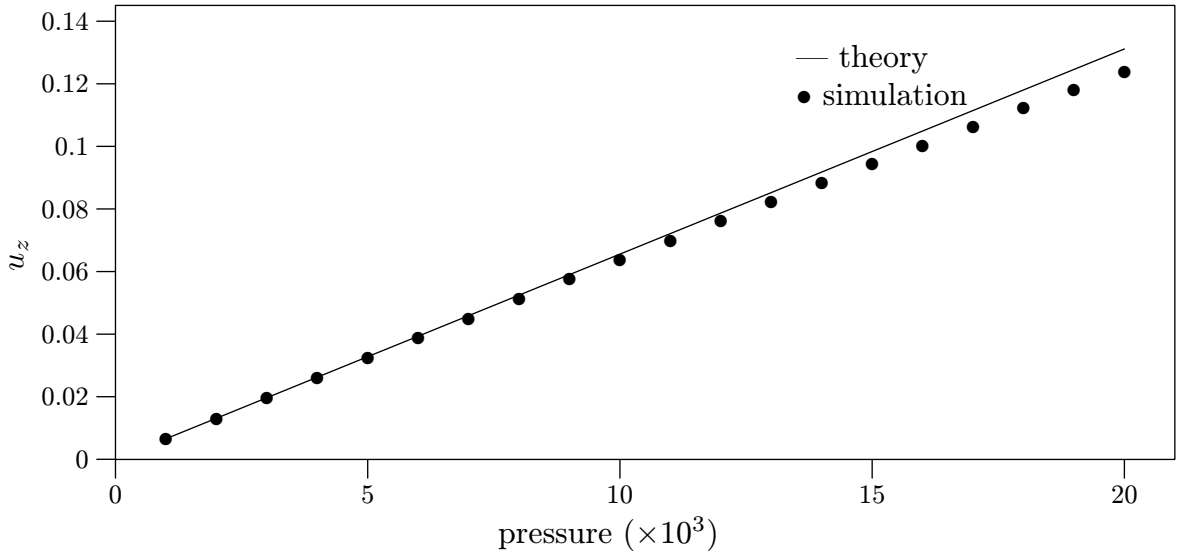

Figure 2: Comparision of the displacement u_z from simulations and theoretical prediction.

6. Conclusion

This paper deals with the modelling of the cylinder with microstructure. Microstructure is described with the microstretch theory in which each point of the continuum can translate, rotate and deform uniformly without shear. Basic equtions of the theory are presented and the

weak formulation is derived. The analytical solution of the extension of the linearly elastic isotropic microstretch cylinder is shown. Finite element discretization is described in details. Numerical results are compared to those predicted by theory and the results are satisfactory.

7. Acknowledgement

This work is supported by the research project MŠM 4977751303.

8. References

G. Capriz. *Continua with Microstructure*. 1989.

T. Davis. Algorithm 832: UMFPACK – an Unsymmetric Pattern Multifrontal Method with a Column Pre-ordering Strategy. *ACM Trans. Math. Software*, 2004.

S. De Cicco and L. Nappa. Torsion and Flexure of Microstretch Elastic Circular Cylinders. *International Journal of Engineering Science*, 1997.

A. Eringen. *Microcontinuum Field Theories I: Foundation and Solids*. 1999.

D. Ieşan and L. Nappa. Saint-Venant's Problem for Microstretch Elastic Solids. *International Journal of Engineering Science*, 1994.

D. Ieşan and L. Nappa. Extension and Bending of Microstretch Elastic Circular Cylinders. *International Journal of Engineering Science*, 1995.